YEAST FOR ETHANOL AND CAROTENOID PRODUCTION

A Thesis

by

CLINT CHENG

Submitted to the Office of Graduate and Professional Studies of
Texas A&M University
in partial fulfillment of the requirements for the degree of

MASTER OF SCIENCE

Chair of Committee,	Katy C. Kao
Committee Members,	Arul Jayaraman
	Deborah Bell-Pedersen
Head of Department,	M. Nazmul Karim

May 2015

Major Subject: Chemical Engineering

ABSTRACT

Lignocellulosic biomass is an attractive source of renewable energy. *Saccharomyces cerevisiae* is often a biocatalyst of choice because of its ability to produce ethanol, as well as its robustness to harsh processing conditions. However, by-products from pretreatment and hydrolysis of biomass can have significant inhibitory effects on the growth of *S. cerevisiae* and biofuel production. We utilize the visualization of evolution in real time (VERT) and genome shuffling to generate strains of *S. cerevisiae* with increased growth rates of up to 13% and 100% in the presence of the by-products furfural and 5-(hydroxymethyl) furfural, respectively.

In addition to biofuel production, *S. cerevisiae* is also a major biocatalyst used for production of biochemicals. The various products that it has been engineered to produce includes carotenoids, which has potential nutraceutical benefits. We have previously developed an evolutionary engineering strategy that couples cell survival with increased carotenoids production and successfully developed carotenoids hyper-producing strains. Intercellular accumulation of the product has been observed in these strains, potentially limiting its production. We attempt to use rational engineering to further improve the productivity of the hyper-producing strains by screening for carotenoids exporters that will potentially increase the driving force for carotenoids production and facilitate the development of a two-phase simultaneous fermentation and extraction system. A variety of genes encoding plasma membrane ATP-binding cassette transporters were cloned into overexpression vectors and transformed into carotenoid-

producing yeast. Increased production of the carotenoid β-carotene was observed in a strain containing an overexpression vector for SNQ2.

ACKNOWLEDGEMENTS

I would like to thank my committee chair, Dr. Kao, and my committee members, Dr. Jayaraman, and Dr. Bell-Pedersen, for imparting me with knowledge and guidance through the course of my research.

Thanks also go to my friends and research group members at Texas A&M University who have shown me nothing but kindness.

TABLE OF CONTENTS

Page

Page

LIST OF FIGURES

LIST OF TABLES

1. INTRODUCTION

The yeast *Saccharomyces cerevisiae* (*S. cerevisiae*) has long been utilized as a biocatalyst to generate a multitude of products, ranging from biofuels to pharmaceuticals to food products. The fermentation of renewable feedstock, particularly lignocellulosic biomass, using *S. cerevisiae* has tremendous potential to alleviate the world's energy needs as we steadily deplete our sources of fossil fuels, and as more sustainable and environmentally responsible energy production becomes increasingly desirable [1, 2]. Strains of *S. cerevisiae* have been engineered to produce simple biofuels, such as ethanol, and various fatty acid ethyl esters found in biodiesel [3, 4]. Metabolic engineering of these strains often requires overexpression of endogenous genes involved in the biosynthetic pathway of these products [5]. In contrast to this, many pharmaceutical and nutraceutical applications involve the heterologous expression of genes from other organisms. The production of flavonoids, carotenoids, and Baccatin III have all been facilitated in *S. cerevisiae* by manipulation of the yeast genome to express proteins from other micro-organisms [6-8]. Dietary consumption of flavonoids has the potential to reduce the risk of cardiovascular disease. Furthermore, the consumption of the carotenoid β-carotene has been reported to reduce the risk of certain cancers, and Baccatin III is a precursor of the anti-cancer drug, paclitaxel [8-10].

The relative ease with which researchers are able to manipulate the genome of *S. cerevisiae*, the abundance of tools and information available on the organism, and its status as being generally regarded as safe, make it an attractive choice of biocatalyst.

However, many challenges in the production of chemicals using *S. cerevisiae* still need to be addressed in order to increase the economic viability of these processes. For example, harsh fermentation conditions, the presence of toxic compounds, and physical limitations of the organism, can all contribute to low productivity and yield [11-13].

My work focuses on overcoming challenges in two aspects of bio-based production in *S. cerevisiae*: the increase in tolerance to toxic hydrolysates present during fermentation of lignocellulosic biomass, and rational metabolic engineering of carotenoid hyper-producing strains of yeast for more efficient extracellular secretion.

Enhanced strains of *S. cerevisiae* have previously been engineered by Almario *et al.* for tolerance to hydrolysate by-products present in hydrolysates of lignocellulosic biomass [14]. Many of these strains contain vastly different mutational backgrounds. My work aims to utilize genome shuffling to create recombinants of these strains with further improved tolerance and to identify the mutations responsible for such observed phenotypes.

Strains of *S. cerevisiae* have also been engineered for the production of carotenoids in our lab [7]. Previous work by Reyes *et al.* have utilized adaptive laboratory evolution to increase carotenoid production. However, further increase in productivity is still necessary for industrial application [11]. Intracellular accumulation of carotenoids have been observed in these strains, with miniscule levels of carotenoids observed in the surrounding growth media. Some gene expression data from the same works suggest this accumulation may have toxic effects on yeast cells. My work aims to amplify the expression of genes that may be involved in the trans-membrane transport of

carotenoids to alleviate these toxic effects and improve production. Furthermore, extracellular export of the desired products may simplify down-stream processing for industrial application.

2. LITERATURE REVIEW

2.1 Lignocellulosic Hydrolysates

A switch from fossil fuels to alternative energy sources is becoming increasingly desirable as the sources of such fuels are being depleted, and as the environmental consequences of global utilization of a non-sustainable energy sources becomes more apparent. Renewable biofuel production shows great promise in attenuating our energy needs in an environmentally conscious way. However, the use of food crops such as corn for such production poses ethical concerns in creating a tradeoff between food supply and energy generation. The use of lignocellulosic biomass would forgo this issue, as well as contribute other ecological benefits: carbon sequestration in soil, minimal nitrous oxide emission, nitrogen and phosphorus conservation, and increased agricultural biodiversity [15, 16]. The ability of some lignocellulosic feed stocks to grow on otherwise marginalized lands can also decrease competition for land and increase the economic feasibility for biofuel production while minimizing habitat destruction and the carbon debt associated with land clearing for feedstock production [17].

Lignocellulosic biomass is made up of three primary components: cellulose, hemicellulose, and lignin. Cellulose is a straight-chain polysaccharide comprised completely of D-glucose subunits. Hemicellulose is a highly branched polysaccharide containing a variety of hexose and pentose subunits. Furthermore, the sugar backbone of

hemicellulose can contain acetyl side groups and other non-sugar compounds. Lignin is a polymer containing a variety of aromatic alcohol subunits which can form a coating around the previously mentioned polysaccharides.

Biofuel production from lignocellulosic biomass requires pretreatment steps to convert polysaccharides into fermentable sugar monomers. A common pretreatment method is dilute acid hydrolysis followed by enzymatic hydrolysis [18]. Dilute acid pretreatment serves to reduce the crystallinity of cellulose and to partially hydrolyze the polysaccharides. Disrupting the ordered arrangement of the cellulose increases its porosity and effective surface area for further hydrolysis. The acid treatment alone can hydrolyze some fraction polysaccharides, however to further increase monomeric conversion, acid treatment is typically followed by enzymatic catalysis with cellulases [19]. Pretreated biomass is then used as a feedstock and converted to biochemical or biofuel products through fermentation with a biocatalyst.

Dilute acid pretreatment, however, can generate a variety of undesirable by-products. Major classes of by-products present include furans, organic acids, and phenolics. Pentose and hexose sugars can be hydrolyzed to furfural and 5-(hydroxymethyl) furfural (HMF), respectively, making these the most abundant furans present after dilute acid hydrolysis as well as other pretreatment methods [20]. Functional groups present on the sugar backbone of hemicellulose can also be liberated during pretreatment. Significant amounts of acetylated hemicellulose results in high levels of acetic acid released during the pretreatment process.

2.2 Yeast Evolution

The baker's yeast *S. cerevisiae* is used in numerous applications in academia as well as in industry. Owing to its high productivity and yield, *S. cerevisiae* is often the biocatalyst of choice for the conversion of lignocellulosic biomass to ethanol [19]. However, a by-products present in pretreated lignocellulosic biomass can inhibit growth of *S. cerevisiae* and ethanol production[12]. In particular, HMF, furfural, and acetic acid can be present in inhibitory concentrations. An increased level of tolerance to these inhibitors is desired as it may aid the proliferation of *S. cerevisiae* and ethanol production.

Adaptive laboratory evolution is a frequently utilized method in biotechnological engineering [21]. In adaptive laboratory evolution, organisms of interest are cultured in conditions that select for desired attributes. Strains containing beneficial mutations outcompete other strains within the same population and can increase in frequency to dominate the population. Using this strategy, *S. cerevisiae* has been evolved by Almario *et al.* in the presence of lignocellulosic hydrolysates by serial passaging over many generations to allow for the selection of mutants with enhanced adaptation to hydrolysates of corn stover [14].

Evolutionary landscapes can be complex and an adaptive laboratory evolution experiment can contain more information than just the mutations that have fixed in the population at the end of the experiment. In large populations, the probability of multiple beneficial mutations arising in independent lineages is high. In asexually reproducing

populations, recombination between sub-populations with different beneficial mutations cannot occur, resulting in competition between these separate lineages. In a phenomena termed clonal interference, these adept sub-populations compete with one another, and the less competitive sub-populations may be driven to extinction [22].

The rational engineering of strains for desired traits requires knowledge on the genes and mechanisms involved, which makes adaptive laboratory evolution a powerful technique for use in inverse strain engineering. The evolved mutants can be readily sequenced using next generation sequencing (NGS) technologies to identify the underlying mutations. However, traditionally, strains are isolated from the end of, or periodically throughout, adaptive laboratory evolution experiments. Any beneficial mutations that had become extinct prior to the points of sampling would not be identified. To help alleviate this limitation, the Visualizing Evolution in Real-Time (VERT) method was developed by our lab. In VERT, multiple fluorescent markers are used to track distinct lineages within the evolving population to characterize the growth dynamics of these independent sub-populations in evolution experiments [23]. *S. cerevisiae* was engineered to express either green, red, or yellow fluorescent proteins to generate three otherwise isogenic strains. Equal proportions of these three strains are used to seed a bioreactor for adaptive laboratory evolution experiments. The evolving population are then sampled regularly (*e.g.* daily) as the evolution experiment proceeds and then analyzed through fluorescence-activated cell sorting (FACS), quantifying the relative abundance of each labeled sub-population. Observed expansions of a colored sub-population suggest the presence of an adaptive mutants within that sub-population;

such expansions are referred to as adaptive events. The data generated allows for characterization of clonal interference events occurring between sub-populations and allows for more rational identification of generations that may contain useful information for subsequent molecular and phenotypic analysis.

In prior work, Almario *et al.* successfully evolved strains of *S. cerevisiae* that were tolerant to hydrolysates generated from dilute acid pretreated corn stover and utilized VERT to identify a number enhanced strains with different mutational backgrounds [14].

2.3 Carotenoid Production in Yeast

Carotenoids belong to a broad class of chemical compounds. Among those considered the most biologically significant to humans are lutein, lycopene, and the various forms of carotene. The benefits associated with carotenoids are typically associated with their ability to mitigate the effects of reactive oxygen species [24]. Carotenoids have been linked to reduced risk of lung cancer and cardiovascular disease, protection against skin damage from sun exposure, and have been used for cosmetics and food coloring [25-29]. β-carotene is also a precursor of vitamin A, and food crops fortified with β-carotene have been engineered to alleviate vitamin A deficiencies [30].

Currently, carotenoids are produced through chemical synthesis or plant extraction [31]. However, production through microbial cell factories may be an attractive option to improve sustainability and economic feasibility. A number of

microorganisms are naturally capable of producing carotenoids, but not at high enough yields to compete with alternative methods. Among these organisms is the red yeast, *Xanthophyllomyces dendrorhous.* The biosynthetic genes responsible for the production of carotenoids have been identified and successfully expressed in *S. cerevisiae* to produce greater amounts of carotenoids, specifically β-carotene [7].

Since rational engineering of strains require *a priori* knowledge of the genes and mechanisms involved, it is likely that there exist gene(s) outside the direct carotenoids biosynthetic pathway that are important for the productivity of these compounds. To further increase carotenoid production, Reyes *et al.* utilized adaptive laboratory evolution and VERT to generate carotenoid hyper-producing strains using hydrogen peroxide as a source of oxidative stress and selective pressure [11]. This strategy allowed us to couple carotenoid production with cell survival, owing to the anti-oxidative properties of the desired compounds.

Microscopic inspection suggested that the vividly colored carotenoids are partitioning to the membranes of the cell, perhaps due to the hydrophobicity of the compounds. Furthermore, analysis of a two phase liquid culture of media and dodecane exhibited very low levels of carotenoid secretion into the dodecane phase, suggesting intracellular localization.

Transcriptome analysis revealed an up-regulation of *PDR3* in a number of the hyper-producing strains; PDR genes have been associated with transmembrane transport of toxic compounds and response to membrane damage via screening of overexpression using high copy-number plasmids or promoter induction, loss of function mutations, and

mutation mapping [32-36]. These data suggested that the accumulation of carotenoids within a cell may inhibit growth.

These observations suggest that extracellular export of carotenoids may serve to increase the driving force for carotenoid production as well as facilitate the downstream development of a two phase simultaneous fermentation and extraction system.

2.4 Gene Targets for Carotenoid Export

A number of genes encoding plasma membrane ATP-binding cassette transporters that are associated with carotenoids have been previously annotated. The genes *PDR5*, *PDR15*, and *SNQ2* have been implicated in cellular responses to high levels of carotenoid production, and are thought to maintain membrane functionality via the export of toxic compounds [37]. *STE6* is known to export the mating pheromone a-factor only after its isoprenylation by carotenoid-like compounds [38]. *YOR1* is known to export various organic compounds, and its overexpression in response to the terpenoid-phenol carvacrol has been observed [39]. In contrast, *PDR11* facilitates the uptake of sterols when native ergosterol synthesis, which, like carotenoid synthesis is derivative of the mevalonate pathway, is compromised [40].

3. MATERIALS AND METHODS

3.1 Strains

Table 1. Strains

Name	**Relevant Features**	**Source**
FY2	*S. cerevisiae,* MATα, ura3-52, S288C background	Kao *et al.* [23]
PG-132	*S. cerevisiae,* FY2 background, hydrolysate evolved mutant	Almario *et al.* [14]
PR-164	*S. cerevisiae,* FY2 background, hydrolysate evolved mutant	Almario *et al.* [14]
PG-259	*S. cerevisiae,* FY2 background, hydrolysate evolved mutant	Almario *et al.* [14]
PG-353	*S. cerevisiae,* FY2 background, hydrolysate evolved mutant	Almario *et al.* [14]
PR-438	*S. cerevisiae,* FY2 background, hydrolysate evolved mutant	Almario *et al.* [14]
GFP-RFP	FY2 background diploid with GFP, RFP	This work
PG-132-RFP	PG-132, FY2-RFP diploid	This work
PR-164-GFP	PG-164, FY2-GFP diploid	This work

Table 1. Continued

Name	**Relevant Features**	**Source**
PG-259-GFP	PG-259, FY2-GFP diploid	This work
PG-353-RFP	PG-353, FY2-RFP diploid	This work
PR-438-GFP	PR-438, FY2-GFP diploid	This work
GSY1136	*S. cerevisiae*, S288C background, MATα, ura3-52, GAL+, YBR209W::Act1p-GFP-Act1t-URA3	Kao *et al.* [23]
YLH2	*S. cerevisiae*, GSY1136 background, carotenoid producing cassette YIplac211YB/I/E*, ΔCTT1	Reyes *et al.* [11]
SM14	*S. cerevisiae*, Hydrogen peroxide evolved strain, derivative of YLH2	Reyes *et al.* [11]
SM14-ATA	SM14, pAG26::TDH3p::ACT1t	This work
SM14-ATA-Snq2	SM14, pAG26::TDH3p::SNQ2::ACT1t	This work
SM14-ATA-Ste6	SM14, pAG26::TDH3p::STE6::ACT1t	This work
SM14-ATA-Yor1	SM14, pAG26::TDH3p::YOR1::ACT1t	This work
BW25113	Laboratory strain of *Escherichia Coli (E. coli)*	Datsenko *et al.* [41]
BW-ATA	BW25113, pAG26::TDH3p::ACT1t	This work
BW-ATA-Snq2	BW25113, pAG26::TDH3p::SNQ2::ACT1t	This work
BW-ATA-Ste6	BW25113, pAG26::TDH3p::STE6::ACT1t	This work
BW-ATA-Yor1	BW25113, pAG26::TDH3p::YOR1::ACT1t	This work

Table 1 contains strains and derivative strains used in this work.

3.2 Materials

The yeast strains were cultured in yeast nitrogen base (YNB) containing 20 g/L dextrose, 1.7 g/L yeast nitrogen base (without amino acids or ammonium sulfate), 5 g//L ammonium sulfate, or yeast extract peptone dextrose (YPD) media containing 20 g/L dextrose, 10 g/L yeast extract, and 20 g/L peptone. Sporulation of yeast was induced with the sporulation medium SPO++ containing 06.25 g/L yeast extract, 37.5 g/L potassium acetate, 450 mg/L adenine, 450 mg/L uracil, 450 mg/L tyrosine, 200 mg/L histidine, 200 mg/L leucine, 200 mg/L lysine, 200 mg/L tryptophan, 200 mg/L methionine, 200 mg/L arginine, 200 mg/L phenylalanine, 350 mg/L threonine, and 5g/L glucose.

E. coli strains were routinely cultured in Lysogeny broth (LB) media containing 10 g/L tryptone, 5 g/L yeast extract, and 10 g/L NaCl. Super optimal broth with catabolite repression (SOC) media containing 20 g/L tryptone, 5 g/L yeast extract, 0.5 g/L NaCl, 0.186 g/L KCl, 0.952 g/L $MgCl_2$, and 3.6 g/L dextrose was used during *E. coli* transformation.

For agar plates, the respective media was supplemented with 20 g/L agar. Cryogenically preserved strains were frozen at -80ºC in media and 17% (v/v) glycerol.

3.3 Primers and Plasmids

Table 2. Primer Sequences for Cloning and Verification of Constructions. Underlined sequences are cut sites for the enzymes in the name of the primer.

Name	**Sequence (5'→ 3')**	**Use**
SalI-ACT1t-f	TCATGTCGACGTAGAAAAGGGAGAGACAAAACACA	Forward primer to amplify ACT1t from FY2, to amplify overlap PCR, and to verify ligation of genes to ACT1t
AvrII-NheI-XbaI-XhoI -ACT1t-r	GTCTAGAGCTAGCCCCTAGGACAAGAATACGACGAAAGTGGTCC	Reverse primer to amplify ACT1t from FY2
AscI-TDH3p-f	TGAGGGCGCGCCCCAATACGCAAACCGCCTCT	Forward primer to amplify TDH3p from yEpGAP plasmid and to amplify overlap PCR
AvrII-NheI-XbaI-XhoI-TDH3p-r	CCTAGGGGCTAGCTCTAGACTCGAGGTCTACCTTCACCTTCACCTTCA	Reverse primer to amplify TDH3p from yEpGAP plasmid
XhoI-PDR5-f	TGAGCTCGAGTGGCTGTTCGCTTTTATTATCA	Forward primer to amplify PDR5 from FY2
NheI-PDR5-r	TGAGGCTAGCTCCATTGCGTCCTTTCTTTTT	Reverse primer to amplify PDR5 from FY2
XhoI-PDR11-f	TGAGCTCGAGTCTAACGGAACGCTATTCACTG	Forward primer to amplify PDR11 from FY2
NheI-PDR11-r	TGAGGCTAGCTGCTGCGGTTTTTGTTTGGC	Forward primer to amplify PDR11 from FY2

Table 2. Continued

Name	**Sequence (5'→ 3')**	**Use**
XbaI-PDR15-f	TGAGTCTAGAACACACACAAGCAAACACACT	Forward primer to amplify PDR15 from FY2
AvrII-PDR15-r	TGAGCCTAGGACGAAAAGAGCCTGATGTTGAA	Forward primer to amplify PDR15 from FY2
XhoI-SNQ2-f	TGAGCTCGAGACTATATCGAAGACCGAAAGCA	Forward primer to amplify SNQ2 from FY2
NheI-SNQ2-r	TGAGGCTAGCTCTGAAGCCCACATTACTGC	Forward primer to amplify SNQ2 from FY2
XhoI-STE6-f	TGAGCTCGAGTGGGTTTAACTGCTTTGGTTGGA	Forward primer to amplify STE6 from FY2
NheI-STE6-r	TGAGGCTAGCAGAGCTTTCAAGTGCCGCTG	Forward primer to amplify STE6 from FY2
XhoI-YOR1-f	TGAGCTCGAGTCAAAAAGAGTAAAGCCGTTGC	Forward primer to amplify YOR1 from FY2
NheI-YOR1-r	TGAGGCTAGCAATGAAAAAGGACCGAAGGCGT	Forward primer to amplify YOR1 from FY2
PDR5-verification-f	AGAGTGCCTAAAAAGAACGGT	Forward primer to verify ligation of PDR5 to ACT1t

Table 2. Continued

Name	**Sequence (5'→ 3')**	**Use**
PDR11-verification-f	ATTGAACGGTAGCCCCATCA	Forward primer to verify ligation of PDR11 to ACT1t
PDR15-verification-f	GGTATCCACCACCAATGCCT	Forward primer to verify ligation of PDR15 to ACT1t
SNQ2-verification-f	CAACCCACCAAACGGCTCAA	Forward primer to verify ligation of SNQ2 to ACT1t
STE6-verification-f	TGCCCGTCAGGATAGAAGTAA	Forward primer to verify ligation of STE6 to ACT1t
YOR1-verification-f	AGAAGGGTGAAGTCGCAGAA	Forward primer to verify ligation of YOR1 to ACT1t
PG-132.1-f	GCCAGCTGATTCTCTTCTTAC	Screening for mutations in diploids
PG-132.1-r	CAGACAAATGGAAGTGGGTTC	Screening for mutations in diploids
PG-132.2-f	CTGCCCTTAATACATACGTTATAC	Screening for mutations in diploids
PG-132.2-r	CATTGCTCTGAGGGCTCATAAC	Screening for mutations in diploids
PG-132.3-f	TCCATTAACGACTTTGACGTC	Screening for mutations in diploids

Table 2. Continued

Name	**Sequence (5'→ 3')**	**Use**
PG-132.3-r	GCGTTTGTGACAAGAAGTAATG	Screening for mutations in diploids
PG-132.4-f	CAATGTCCAGTTGAGCCACC	Screening for mutations in diploids
PG-132.4-r	CAGAAGAAGTATTCGAACTGAGG	Screening for mutations in diploids
PG-164.1-f	TGATCCCACCACCATGGTC	Screening for mutations in diploids
PG-164.1-r	TGATCCCACCACCATGGTA	Screening for mutations in diploids
PG-259.1-f	CGCTCTCATGGGTCAAGATAA	Screening for mutations in diploids
PG-259.1-r	AGGTAGAAGAGGGTCAGCAC	Screening for mutations in diploids
PG-259.2-f	CTACGCATATGGTTTCAAGATC	Screening for mutations in diploids
PG-259.2-r	GTACCACCAGTGGATTGCAC	Screening for mutations in diploids
PG-259.3-f	GCCAGATCCAAAGTAGCCTTAG	Screening for mutations in diploids

Table 2. Continued

Name	**Sequence (5'→ 3')**	**Use**
PG-259.3-r	CGATTGACACAGAGGCATGTTC	Screening for mutations in diploids
PG-259.4-f	GCCTTCTGCCAAAGAGGTTAA	Screening for mutations in diploids
PG-259.4-r	AGACATATTAGGCATCAGAGG	Screening for mutations in diploids
PG-259.5-f	GCGCTAGGGTGAAGAGAGTTA	Screening for mutations in diploids
PG-259.5-r	GTTGTTGGCGTGTGCATTT	Screening for mutations in diploids
PG-259.6-f	GACATTGTTTCCGTAGCTTTA CC	Screening for mutations in diploids
PG-259.6-r	TATGCACGCTCCACTTACTCC	Screening for mutations in diploids
PG-353.1-f	TCTTGTTGGGCGAAAACAGAG	Screening for mutations in diploids
PG-353.1-f	TGAAAATTATCCTGGGCTGCA	Screening for mutations in diploids
PR-438.1-f	GACTTCAATACAGTCTTCGAAC CAAA	Screening for mutations in diploids

Table 2. Continued

Name	**Sequence (5'→ 3')**	**Use**
PR-438.1-r	TCCTTATACAGCTGCTGTTACA AT T	Screening for mutations in diploids
PR-438.2-f	GACTTCAATACAGTCTTCGAAC CAAC	Screening for mutations in diploids
PR-438.2-r	TCCTTATACAGCTGCTGTTACA AT T	Screening for mutations in diploids

Table 2 contains various oligonucleotides used for genetic manipulation in these works.

The TDH3p (TDH3 promoter) sequence was amplified from the plasmid yEpGAP-cherry [42]. The yeast centromere plasmid pAG26 was the vector used for cloning [43]; it contains hygromycin resistance B marker (hph), ampicillin resistance marker (amp), and uracil biosynthesis marker (URA3).

3.4 Mating

Standard yeast mating and zygote-pulling using a micro-dissection procedure were used to generate the heterozygous diploid strains of each evolved mutant PG-132, PG-259, PG-353, PR-164, and PR-438. These haploid strains were mated with wild-

type strains of FY2 marked with a different fluorescent proteins. An FY2 strain with a GFP marker and a FY2 strain with an RFP marker were also mated to generate the GFP-RFP reference diploid strain. The strains to be mated were grown overnight in YPD media. 250 µl of the overnight culture of each strain were combined in a sterile 1.5 mL microcentrifuge tube. 10 µl of each mixed culture were spotted on YPD plate and incubated at 30ºC for two hours to allow mating. A small portion of the cells were inspected under the microscope for zygote formation. If the formation of zygotes was observed, at least five of these zygotes were pulled using a micromanipulator. The resulting diploids were verified using flow cytometry (FACScan). Diploids products for each isolated mutant were named PG132-RFP, PG259-RFP, PR438-GFP, PR164-GFP and PG353-RFP. Sporulation was induced with SPO++ media in separate test tubes for each diploid. Once sporulation was observed, the spore sacs were digested with zymolyase and the spore mixture from all five strains (PG132-RFP, PG259-RFP, PR438-GFP, PR164-GFP and PG353-RFP) were combined in one test tube. The resulting mixture was then plate on YPD plates at 30ºC to allow for massive mating overnight.

3.5 Enrichment

After incubation, cells were transferred to a synthetic hydrolysate media with concentration of 1.44g/L HMF, 0.036g/L furfural and 14.4 mM acetic acid in YNB. The cells were serially passaged daily in fresh synthetic hydrolysates for the course of three days. On the fourth day, cells were plated on solid media of synthetic hydrolysates and

agar. Approximately 20 colonies that grew on plates were cultured with this synthetic hydrolysate media on a 96 well plate in a TECAN™ Infinite M200 microplate reader. The four recombinants with the greatest specific growth rates were named PMM1, PMM2, PMM3, and PMM4.

3.6 Growth Kinetics

The wild-type diploid GFP-RFP, the five hydrolysate evolved mutant diploids, and the four potential recombinants were revived from frozen stocks by plating on YPD agar plates and incubated at 30°C for approximately 70 hours. At least four colonies per condition of each strain were chosen based on normal size and appearance and grown in test tubes for approximately 14 hours with 2mL of YNB media supplemented with 1% (w/v) glucose and the following conditions: (a) no hydrolysates, (b) 40mM acetic acid, (c) 0.7 g/L furfural, (d) 0.9 g/L HMF, (e) 8.8mM acetic acid, 0.022 g/L furfural, and 0.88 g/L HMF. These conditions were determined after observing growth in a gradient of concentrations (data not shown) and selecting concentrations high enough to inhibit growth of the GFP-FP but not completely prevent its growth. For condition (e), relative amounts of each inhibitor chosen were based on the highest levels of each inhibitor previously observed in various batches of pretreated corn stover [14]. 5 uL of each culture was used to inoculate 100 µL of fresh YNB media supplemented with 1% (w/v) glucose and the corresponding inhibitory condition. Cultures were grown in 96 well plates with at least two technical replicates per biological replicate. OD600 was

monitored every 10 minutes using a TECAN^{TM} Infinite M200 microplate reader at 30°C with a 2 mm orbital amplitude for up to 34 hours.

The specific growth rates were calculated by finding the maximum difference between the logs of two OD600 measurements seven data points apart and dividing by the elapsed time. A least squared linear regression was applied to these seven data points. If R^2 values were greater than 0.997, the number of selected data points would expand by two and iteratively analyzed in this way until R^2 dropped below the chosen threshold of 0.997. The slope of the linear fit of the resulting data set was taken as the maximal specific growth rate. If the R^2 of the initial seven data points is less than 0.997, the number of selected data points would be expanded by two iteratively so long as expansion resulted in an increase in R^2. Outlying data points were detected by comparing specific growth rates calculated this way to the specific growth rate calculated by slope between the initial seven data points. When outlying data points were detected, ranges for locating maximal differences were manually altered to avoid erroneous data. When the iterative expansion of data points resulted in use of data from the latest time point in a TECAN run, growth curves were labeled as not reaching stationary phase.

The relative fitness coefficients were calculated for each strain using the following equation.

$$\frac{\mu_{\mathbf{mutant_i}}}{\mu_{\mathbf{wildtype_i}}} - \mathbf{1}$$

The symbol μ is the specific growth rate of the strain under the various inhibitory conditions. A specific fitness coefficient was calculated with the following equation.

$$\frac{\left(\frac{\mu_{\text{mutant}_i}}{\mu_{\text{mutant}_0}} - \frac{\mu_{\text{wildtype}_i}}{\mu_{\text{wildtype}_0}}\right)}{\frac{\mu_{\text{wildtype}_i}}{\mu_{\text{wildtype}_0}}}$$

The subscripts "i" and "o" denote the presence of inhibitors or lack thereof, respectively.

3.7 Genome Sequencing

The genomes of the original isolated evolved haploid mutants (PG-132, PG-259, PG-353, PR-164, and PR-438) were sequenced using Illumina HiSeq 2500 with 100 base-pair single-end reads. CLC Workbench was used to analyze the data using default threshold levels. Each sequence was aligned to the reference *S. cerevisiae* strain S288C. The parental strain was also sequenced to eliminate any differences between the S288C strain used in our studies and the reference S288C sequence in the database. Differences between the alignment of the parental strain and evolved strains were used to identify mutations and verified via Sanger sequencing.

3.8 Construction of Yeast Strains with Transporter Overexpression Plasmids

S. cerevisiae strain FY2 was grown in YPD media for approximately 24 hours at 30ºC with agitation. Genomic DNA was isolated from these cells using ZR Fungal/Bacterial DNA MiniPrep™ kit (Zymo Research). Genes of interest and the

ACT1 terminator (ACT1t) were PCR amplified from the wild-type genomic DNA using a high fidelity DNA polymerase and the corresponding primers, i.e. XhoI-PDR5-f and NheI-PDR5-r for PDR5 (Table 2). The PCR products for each gene-of-interest were digested with corresponding enzymes, *e.g.* PDR5 was digested with XhoI and NheI. The TDH3 promoter (TDH3p) was used to express the transporters and was amplified from plasmid yEpGAP-cherry using the primers AscI-TDH3p-f and AvrII-NheI-XbaI-XhoI-TDH3p-r. Overlap extension PCR was used to generate a construct containing the TDH3p and the ACT1t with a multiple cloning site between them (TDH3p::ACT1t). TDH3p::ACT1t and the plasmid pAG26 were digested with AscI and SalI and ligated with T4 DNA ligase. The ligated product (pAG26::TDH3p::ACT1t) was transformed into the *E. coli* strain BW25113 using an electroporation protocol [44]. Cells were cultured in SOC media for approximately one hour and plated on LB agar plates supplemented with 100 µg/mL ampicillin. Correct transformants were verified using colony PCR with AscI-TDH3p-f and SalI-ACT1t-r. A successful transformant was cultured in LB media supplemented with 100 µg/mL ampicillin for approximately 24 hours. Plasmid DNA was isolated from these cells and digested with enzymes corresponding to the respect gene of interest, *e.g.* XhoI and NheI for PDR5, and then ligated with the corresponding gene of interest. The ligated product was transformed into BW25113 and cultured as previously stated. Transformants were verified using colony PCR with SalI-ACT1t-f and the corresponding verification primer, *e.g.* PDR5-verification-f for PDR5. The resulting plasmid was transformed into yeast strain SM14 using the lithium acetate method with salmon sperm DNA, and PEG 3350 [45].

Transformants were selected for on YNB plates supplemented with 400 µg/mL Hygromycin B and verified with colony PCR as previously stated.

3.9 Carotenoid Export

SM14-ATA, SM14-Snq2, SM14-Ste6, and SM14-Yor1 were cultured in a two-phase liquid culture of 30 mL YPD overlayed with 15 mL of dodecane at 30°C for roughly three days. 200 µL of the dodecane phase was plated in a 96 well plates with opaque walls and a clear bottom. Absorbances were measured in a TECAN™ Infinite M200 microplate reader with wavelengths ranging from 350 nm to 550 nm in 2 nm intervals. Relative amounts of carotenoids were estimated from the area under the spectral curve using the trapezoidal rule and compared to the reference strain SM14-ATA. β-carotene concentrations were quantified using a standard curve generated by β-carotene obtained from Enzo Life Sciences (Supplementary Materials.)

4. RESULTS

4.1 Yeast Tolerance to Lignocellulosic Hydrolysates

Growth Rate in Presence of Inhibitors

Massive mating of our previously evolved mutants (PG-132, PG-259, PG-353, PR-164, and PR-438) allows for genetic recombination and has the potential to generate more fit recombinants. Heterozygous diploids of each of the five previously evolved haploid strains of *S. cerevisiae* were generated by mating each haploid with a wild-type strain marked with a different fluorescent protein. The resulting diploids were sporulated and mass mated to generate recombinants. The resulting mating products were enriched through serial passage in media containing a mixture of HMF, furfural, and acetic acid. The best performing strains were named PMM1, PMM2, PMM3, and PMM4.

These potential diploid recombinants were phenotypically characterized under a variety of conditions along with their parental heterozygous diploid strains (PG132-RFP, PG259-RFP, PR438-GFP, PR164-GFP and PG353-RFP). None of the parental strains exhibited significant increase in specific growth rate relative to the wild-type GFP-RFP (Supplemental Material.) PMM1 exhibited a 13% increase in fitness relative to GFP-RFP in the presence of furfural (Figure 1). PMM3 and PMM4 exhibited a 37% and 100% increase in relative fitness in the presence of HMF, respectively. PMM4 also

exhibited a 30% increase in relative fitness in the presence of a mixture of furfural, HMF, and acetic acid with a p-value of 0.056.

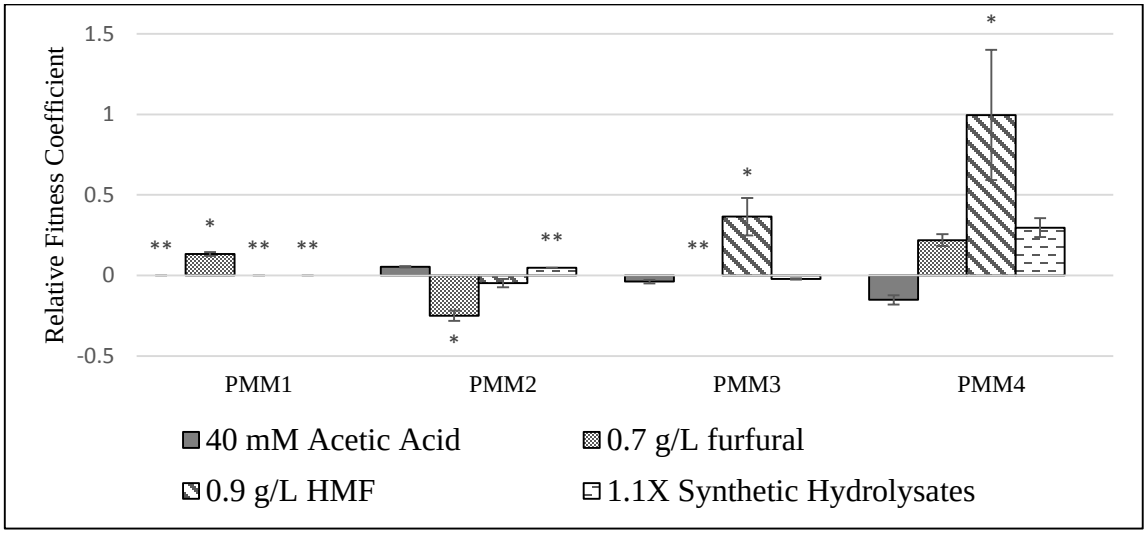

Figure 1. Relative Fitness of Mating Products to Inhibitor Conditions. Specific growth rates of each mating product relative to GFP-RFP in the presence of individual inhibitors and in a mixture of all three. Asterisk indicates statistical significance between mating products and GFP-RFP with a P-value < 0.05 (two-tailed student's t-test, unequal variances.) Two asterisks indicate at least three replicates under this condition were unable to grow or unable to reach stationary phase within 34 hours.

To analyze whether these changes in specific growth rates were unique to their inhibitory condition, rather than a general increase in fitness, we calculated a specific fitness coefficient that compared the difference in growth rate with and without inhibition from the mutant strains to the wild-type diploid GFP-RFP (Figure 2). PMM4 exhibited the highest levels increase in specific growth rate under inhibition compared to growth without inhibition. Its specific fitness coefficients are 1.06 and 0.43 in HMF and

the mixture of the three hydrolysates, respectively. PMM1 and PMM3 exhibit lower levels of relative change in specific growth rates, with specific fitness coefficients of 0.04 in furfural and 0.24 in HMF, respectively.

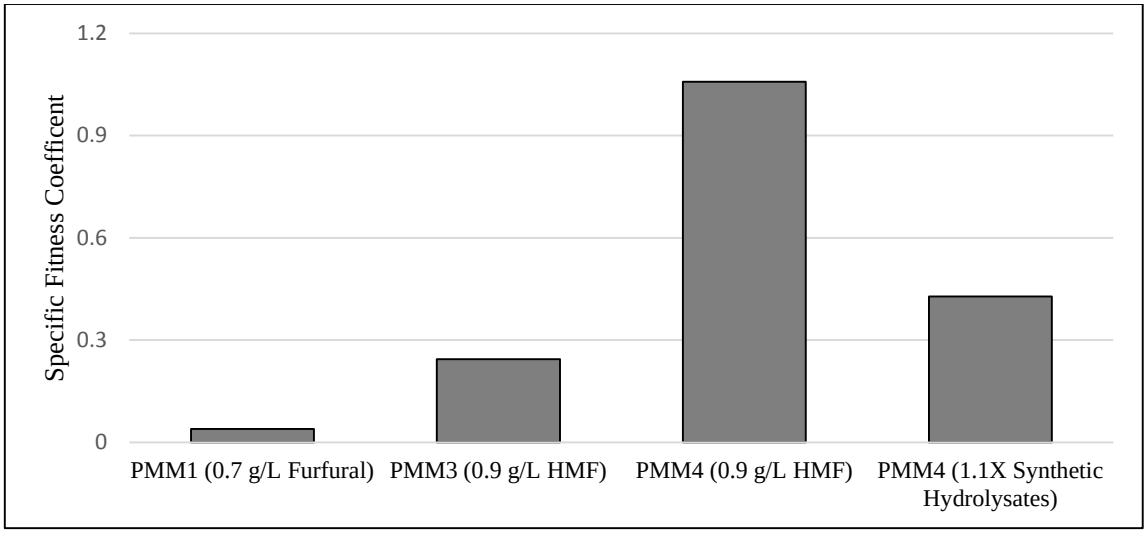

Figure 2. Specific Fitness Coefficients. Change in growth rate with and without inhibition compared to the change in GFP-RFP.

Genomic Analysis

The genomes of the parental haploid strains were sequenced with Illumina HiSeq. Multiple mutations were found in each strain, relative to the wild-type parental strain. Amongst the five strains, eight intergenic mutations were identified with five being single nucleotide polymorphisms (SNPs) and two being insertions of one or four base pairs (Supplemental Material.) One of the SNPs occurred in an autonomously

replicating sequence, ARS300. Nine different SNPs were found in coding regions, all of which were non-synonymous (Table 3).

Table 3. Genes Containing Mutations

PG-132	**PR-164**	**PG-259**	**PG-353**	**PR-438**
ART10	PKP1	ESC2	ESC2	PKP1
SMF1		FLC3	FLC3	COQ5
		COQ6	COQ6	
		SMF1		
		YPR015C		

Sanger sequencing was used to determine which mutations from the original evolved mutants are present in the recombinants (Table 4). The results showed that all identified mutations in the recombinants occurred in coding regions and were non-synonymous.

Table 4. Mutations in Mating Products

	PG-132.2 *ARS300*	**PG-132.3** *ART10*	**PG132.4** *SMF1*	**PG-259.5** *SMF1*
PMM1		Y	Y	Y
PMM2	Y	Y	Y	
PMM3				Y
PMM4	Y	Y	Y	

4.2 Carotenoid Export

Attempts to transform our carotenoid hyper-producing strain, SM14, with overexpression plasmids for PDR5, PDR11, and PDR15 failed after multiple attempts. Correct transformants containing overexpression plasmids for SNQ2, STE6, and YOR1, however, were successfully isolated. These strains were cultured in YPD media overlayed dodecane. Analysis of the organic phase revealed no statistically significant difference in total carotenoid concentration compared to the reference strain containing an empty plasmid, SM14-ATA (Supplementary Material). SM14-ATA-Snq2 did, however, show a significant increase in β-carotene concentration with 4.0 ± 0.4 mg/L as compared to 3.0 ± 0.2 mg/L in the reference strain.

5. CONCLUSION

Genome shuffling between isolated mutants evolved in the presence of hydrolysates of corn stover generated three recombinants (PMM1, PMM3, and PMM4) with increased tolerance to inhibitors. The increase in fitness exhibited by PMM4 in HMF was shown to be specific to the inhibitory condition, whereas the increase in fitness present in PMM1 and PMM3 in furfural and HMF, respectively, are likely attributed to a general increase in fitness. Sequencing data reveals PMM1 and PMM4 are likely progeny of PG-132 but neither carried over one of its intergenic mutations and furthermore PMM1 did not carry over the mutation occurring in ARS300. PMM1 and PMM3 both contained a single mutation in SMF1 from the evolved mutant PG-259 but none of the other six mutations.

It is interesting to note that our best performing recombinant, PMM4, contains only mutations from the evolved mutant PG-132. Amongst the evolved mutants used to generate the recombinants, PG-132 was isolated from the earliest population in the evolution experiment. Furthermore, both PG-132 and PG-259 contain mutations in SMF1 that were present in all of our recombinants, however, the SNP present in PG-132 occurs at a different base-pair than that of PG-259. SMF1 is known to be involved in transport of divalent ions.

The engineered carotenoid producing strain SM14-ATA-Snq2 exhibited increased secretion of β-carotene. Though not statistically significant based on the six technical replicates analyzed, this strain also had an 18% increase in total carotenoid

secretion as compared to the reference strain. Further studies with more biological replicates are necessary to suggest an increase in total carotenoid secretion and to confirm the increase in β-carotene secretion. Additional work may be done to assess the level of transcription of their respective genes in the transformants, SM14-ATA-Snq2, SM14-ATA-Ste6, and SM14-ATA-Yor1, at an RNA level to verify overexpression. Failure to isolate transformants overexpressing PDR5, PDR11, and PDR15 is possibly due to toxicity caused by overexpression. Further cloning with lower copy-number plasmids or weaker promoters may provide further insight into these three genes. Potential gene targets for further rational engineering include the other plasma membrane ATP-binding cassette transporters identified in yeast: PDR10, PDR12, PDR18, AUS1, MDL1, and MDL2. In particular, an up-regulation of PDR10 and PDR18 in response to the presence of the terpenoid phenol carvacrol have been observed [46].

REFERENCES

1. U.S. Department of Energy, *U.S. billion-ton update: biomass supply for a bioenergy and bioproducts industry.* Perlack and B.J. Stokes (Leads), ORNL/TM-2011/224. Oak Ridge National Laboratory, Oak Ridge, TN. 227p.
2. Perlack, R.D., Wright, L. L., Turhollow, A. F., Graham, R. L., Stokes, B. J. and Erbach, D. C. , *Biomass as feedstock for a bioenergy and bioproducts industry: The technical feasibility of a billion-ton annual supply.* (DOE/GO-102995-2135 or ORNL/TM-2005/66), Oak Ridge, TN: Oak Ridge National Laboratory., 2005.
3. Madhavan, A., A. Srivastava, A. Kondo, and V.S. Bisaria, *Bioconversion of lignocellulose-derived sugars to ethanol by engineered* Saccharomyces cerevisiae. Crit Rev Biotechnol, 2012. **32**(1): p. 22-48.
4. Runguphan, W. and J.D. Keasling, *Metabolic engineering of* Saccharomyces cerevisiae *for production of fatty acid-derived biofuels and chemicals.* Metab Eng, 2014. **21**: p. 103-13.
5. Jones, G.M., J. Stalker, S. Humphray, A. West, T. Cox, et al., *A systematic library for comprehensive overexpression screens in* Saccharomyces cerevisiae. Nat Meth, 2008. **5**(3): p. 239-241.
6. Koopman, F., J. Beekwilder, B. Crimi, A. van Houwelingen, R.D. Hall, et al., *De novo production of the flavonoid naringenin in engineered* Saccharomyces cerevisiae. Microb Cell Fact, 2012. **11**: p. 155.

7. Verwaal, R., J. Wang, J.P. Meijnen, H. Visser, G. Sandmann, et al., *High-level production of beta-carotene in* Saccharomyces cerevisiae *by successive transformation with carotenogenic genes from* Xanthophyllomyces dendrorhous. Appl Environ Microbiol, 2007. **73**(13): p. 4342-50.

8. Dejong, J.M., Y. Liu, A.P. Bollon, R.M. Long, S. Jennewein, et al., *Genetic engineering of taxol biosynthetic genes in* Saccharomyces cerevisiae. Biotechnol Bioeng, 2006. **93**(2): p. 212-24.

9. Wang, X., Y.Y. Ouyang, J. Liu, and G. Zhao, *Flavonoid intake and risk of CVD: a systematic review and meta-analysis of prospective cohort studies.* Br J Nutr, 2014. **111**(1): p. 1-11.

10. Goralczyk, R., *Beta-carotene and lung cancer in smokers: review of hypotheses and status of research.* Nutr Cancer, 2009. **61**(6): p. 767-74.

11. Reyes, L.H., J.M. Gomez, and K.C. Kao, *Improving carotenoids production in yeast via adaptive laboratory evolution.* Metab Eng, 2014. **21**: p. 26-33.

12. Li, Q., J. Song, S. Peng, J.P. Wang, G.Z. Qu, et al., *Plant biotechnology for lignocellulosic biofuel production.* Plant Biotechnol J, 2014. **12**(9): p. 1174-92.

13. Favaro, L., M. Basaglia, A. Trento, E. Van Rensburg, M. Garcia-Aparicio, et al., *Exploring grape marc as trove for new thermotolerant and inhibitor-tolerant* Saccharomyces cerevisiae *strains for second-generation bioethanol production.* Biotechnol Biofuels, 2013. **6**(1): p. 168.

14. Almario, M.P., L.H. Reyes, and K.C. Kao, *Evolutionary engineering of* Saccharomyces cerevisiae *for enhanced tolerance to hydrolysates of lignocellulosic biomass.* Biotechnol Bioeng, 2013. **110**(10): p. 2616-23.

15. Robertson, G.P., S.K. Hamilton, S.J. Del Grosso, and W.J. Parton, *The biogeochemistry of bioenergy landscapes: carbon, nitrogen, and water considerations.* Ecol Appl, 2011. **21**(4): p. 1055-67.

16. Gelfand, I., R. Sahajpal, X. Zhang, R.C. Izaurralde, K.L. Gross, et al., *Sustainable bioenergy production from marginal lands in the US Midwest.* Nature, 2013. **493**(7433): p. 514-7.

17. Fargione, J., J. Hill, D. Tilman, S. Polasky, and P. Hawthorne, *Land clearing and the biofuel carbon debt.* Science, 2008. **319**(5867): p. 1235-8.

18. Faith, W.L., *Development of the Scholler Process in the United States.* Industrial & Engineering Chemistry, 1945. **37**(1): p. 9-11.

19. Singh, R., A. Shukla, S. Tiwari, and M. Srivastava, *A review on delignification of lignocellulosic biomass for enhancement of ethanol production potential.* Renewable and Sustainable Energy Reviews, 2014. **32**(0): p. 713-728.

20. van der Pol, E.C., R.R. Bakker, P. Baets, and G. Eggink, *By-products resulting from lignocellulose pretreatment and their inhibitory effect on fermentations for (bio)chemicals and fuels.* Appl Microbiol Biotechnol, 2014. **98**(23): p. 9579-93.

21. Dragosits, M. and D. Mattanovich, *Adaptive laboratory evolution – principles and applications for biotechnology.* Microbial Cell Factories, 2013. **12**: p. 64-64.

22. Lang, G.I., D.P. Rice, M.J. Hickman, E. Sodergren, G.M. Weinstock, et al., *Pervasive genetic hitchhiking and clonal interference in forty evolving yeast populations.* Nature, 2013. **500**(7464): p. 571-4.

23. Kao, K.C. and G. Sherlock, *Molecular characterization of clonal interference during adaptive evolution in asexual populations of* Saccharomyces cerevisiae. Nat Genet, 2008. **40**(12): p. 1499-504.

24. Fiedor, J. and K. Burda, *Potential role of carotenoids as antioxidants in human health and disease.* Nutrients, 2014. **6**(2): p. 466-88.

25. Garcia-Closas, R., A. Agudo, C.A. Gonzalez, and E. Riboli, *Intake of specific carotenoids and flavonoids and the risk of lung cancer in women in Barcelona, Spain.* Nutr Cancer, 1998. **32**(3): p. 154-8.

26. Voutilainen, S., T. Nurmi, J. Mursu, and T.H. Rissanen, *Carotenoids and cardiovascular health.* Am J Clin Nutr, 2006. **83**(6): p. 1265-71.

27. Kopcke, W. and J. Krutmann, *Protection from sunburn with beta-carotene--a meta-analysis.* Photochem Photobiol, 2008. **84**(2): p. 284-8.

28. Fisher, G.J. and J.J. Voorhees, *Molecular mechanisms of retinoid actions in skin.* FASEB J, 1996. **10**(9): p. 1002-13.

29. Gordon, H.T. and J.C. Bauernfeind, *Carotenoids as food colorants.* Crit Rev Food Sci Nutr, 1982. **18**(1): p. 59-97.

30. Paine, J.A., C.A. Shipton, S. Chaggar, R.M. Howells, M.J. Kennedy, et al., *Improving the nutritional value of Golden Rice through increased pro-vitamin A content.* Nat Biotech, 2005. **23**(4): p. 482-487.

31. Alvarez, R., B. Vaz, H. Gronemeyer, and A.R. de Lera, *Functions, therapeutic applications, and synthesis of retinoids and carotenoids.* Chem Rev, 2014. **114**(1): p. 1-125.

32. Jungwirth, H. and K. Kuchler, *Yeast ABC transporters-- a tale of sex, stress, drugs and aging.* FEBS Lett, 2006. **580**(4): p. 1131-8.

33. Carvajal, E., H.B. van den Hazel, A. Cybularz-Kolaczkowska, E. Balzi, and A. Goffeau, *Molecular and phenotypic characterization of yeast PDR1 mutants that show hyperactive transcription of various ABC multidrug transporter genes.* Mol Gen Genet, 1997. **256**(4): p. 406-15.

34. Rank, G.H., A.J. Robertson, and K.L. Phillips, *Modification and inheritance of pleiotropic cross resistance and collateral sensitivity in* Saccharomyces cerevisiae. Genetics, 1975(3): p. 783-93.

35. Katzmann, D.J., P.E. Burnett, J. Golin, Y. Mahe, and W.S. Moye-Rowley, *Transcriptional control of the yeast PDR5 gene by the PDR3 gene product.* Mol Cell Biol, 1994. **14**(7): p. 4653-61.

36. Leppert, G., R. McDevitt, S.C. Falco, T.K. Van Dyk, M.B. Ficke, et al., *Cloning by gene amplification of two loci conferring multiple drug resistance in* saccharomyces. Genetics, 1990. **125**(1): p. 13-20.

37. Verwaal, R., Y. Jiang, J. Wang, J.M. Daran, G. Sandmann, et al., *Heterologous carotenoid production in* Saccharomyces cerevisiae *induces the pleiotropic drug resistance stress response.* Yeast, 2010. **27**(12): p. 983-98.

38. Caldwell, G.A., S.H. Wang, F. Naider, and J.M. Becker, *Consequences of altered isoprenylation targets on a-factor export and bioactivity.* Proc Natl Acad Sci U S A, 1994. **91**(4): p. 1275-9.

39. Rao, A., Y. Zhang, S. Muend, and R. Rao, *Mechanism of antifungal activity of terpenoid phenols resembles calcium stress and inhibition of the TOR pathway.* Antimicrob Agents Chemother, 2010. **54**(12): p. 5062-9.

40. Kuo, D., K. Tan, G. Zinman, T. Ravasi, Z. Bar-Joseph, et al., *Evolutionary divergence in the fungal response to fluconazole revealed by soft clustering.* Genome Biol, 2010. **11**(7): p. R77.

41. Datsenko, K.A. and B.L. Wanner, *One-step inactivation of chromosomal genes in Escherichia coli K-12 using PCR products.* Proc Natl Acad Sci U S A, 2000. **97**(12): p. 6640-5.

42. Keppler-Ross, S., C. Noffz, and N. Dean, *A new purple fluorescent color marker for genetic studies in* Saccharomyces cerevisiae *and* Candida albicans. Genetics, 2008. **179**(1): p. 705-710.

43. Goldstein, A.L. and J.H. McCusker, *Three new dominant drug resistance cassettes for gene disruption in* Saccharomyces cerevisiae. Yeast, 1999. **15**(14): p. 1541-53.

44. Morrison, S.L., *Transformation of E. coli by electroporation.* Curr Protoc Immunol, 2001. **Appendix 3**: p. Appendix 3N.

45. Gietz, R.D. and R.A. Woods, *Transformation of yeast by lithium acetate/single-stranded carrier DNA/polyethylene glycol method.* Methods Enzymol, 2002. **350**: p. 87-96.

46. Rao, A., Y. Zhang, S. Muend, and R. Rao, *Mechanism of antifungal activity of terpenoid phenols resembles calcium stress and inhibition of the TOR pathway.* Antimicrobial Agents and Chemotherapy, 2010. **54**(12): p. 5062-5069.

APPENDIX

SUPPLEMENTARY MATERIALS

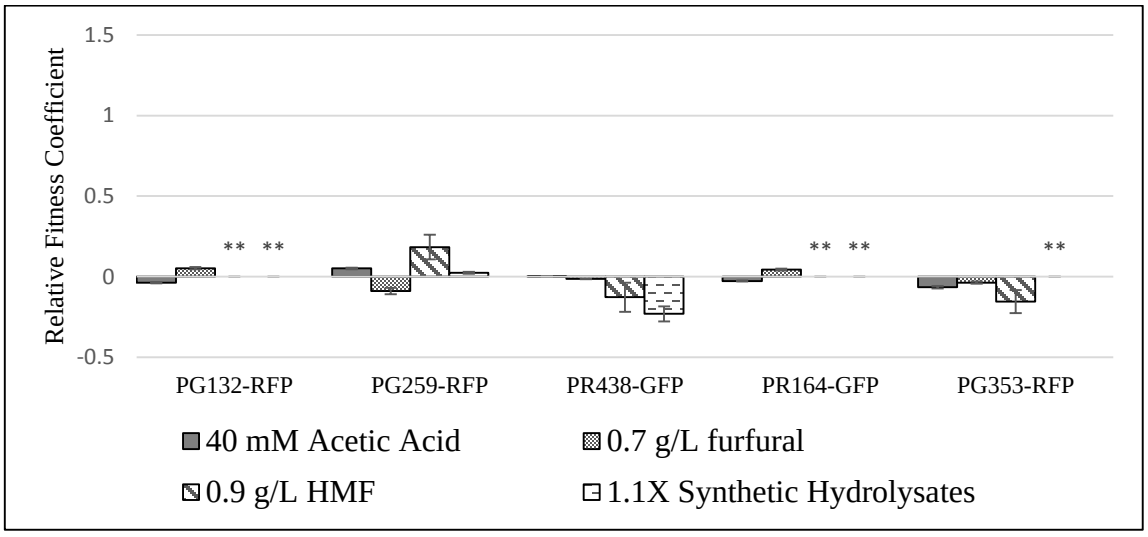

Figure 3. Fitness of Parental Strains Relative to GFP-RFP. Two asterisks denotes that at least three replicates were unable to grow or unable to reach stationary phase within 34 hours. No fitness coefficients were statistically different than that of GFP-RFP with a P-value < 0.05 (two-tailed student's t-test, unequal variances.)

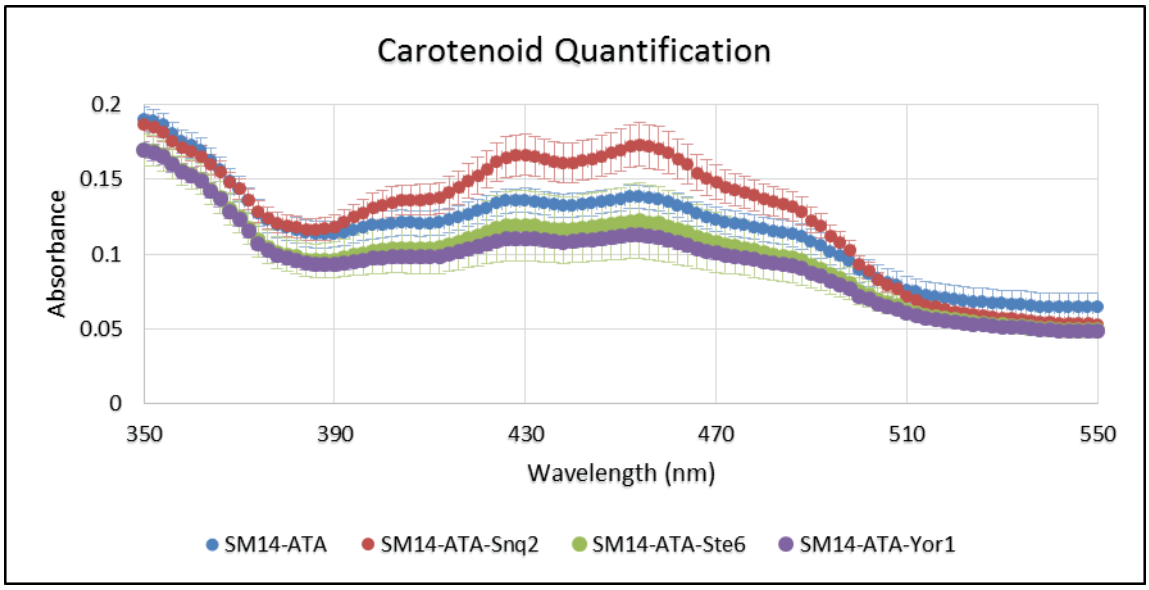

Figure 4. Absorbance across Visible Carotenoid Spectra. Carotenoid concentrations in the dodecane phase of bilayer culture were analyzed across wavelengths where carotenoids show characteristic absorbances.

Table 5. Genome Sequencing Results

Chrom-osome	Strain Number	Position	Ref	Evo	Type	Gene	Amino acid change
II	PG-132.1	353568	C	A		Intergenic	
III	PG-132.2	1158	G	T		ARS300	
XII	PG-132.3	905647	T	A	Missense	ART10	Glu → Val
XV	PG-132.4	91152	A	G	Missense	SMF1	Tyr → His
II	PG259.1	353563	C	A		Intergenic	
IV	PG259.2	1200461	A	C	Missense	ESC2	Leu → Phe
VII	PG259.3	246244	C	G	Missense	FLC3	Thr → Ser
VII	PG259.4	1003785	T	C	Missense	COQ6	Asp → Gly
VIII	PG259.5	391764	-	A	Insertion	Intergenic	
XV	PG259.6	90569	G	A	Missense	SMF1	Ser → Phe
XVI	PG259.7	590694	A	G	Missense	YPR015C	Ser → Pro
IX	PR-438.1	275180	C	A	Missense	PKP1	Asp → Tyr
XIII	PR-438.2	50798	A	C	Missense	COQ5	Phe → Val
IX	PR-164.1	275283	C	A	Missense	PKP1	Asp → Tyr
II	PG-353.1	353553	C	A		Intergenic	
IV	PG-353.2	1200463	A	C	Missense	ESC2	Leu → Phe
VII	PG-353.3	246244	C	G	Missense	FLC3	Thr → Ser
VII	PG-353.4	1003785	T	C	Missense	COQ6	Asp → Gly
VIII	PG-353.5	391764	-	A	Insertion	Intergenic	

Table 6. Carotenoid Quantification. The area under the curve generated by absorbance data ranging from 350 nm to 550 nm were calculated using the trapezoidal rule.

	Average Area Under Curve	Standard Deviation
SM14-ATA	23.11	1.72
SM14-ATA-Snq2	25.17	1.63
SM14-ATA-Ste6	19.84	0.97
SM14-ATA-Yor1	18.98	0.78

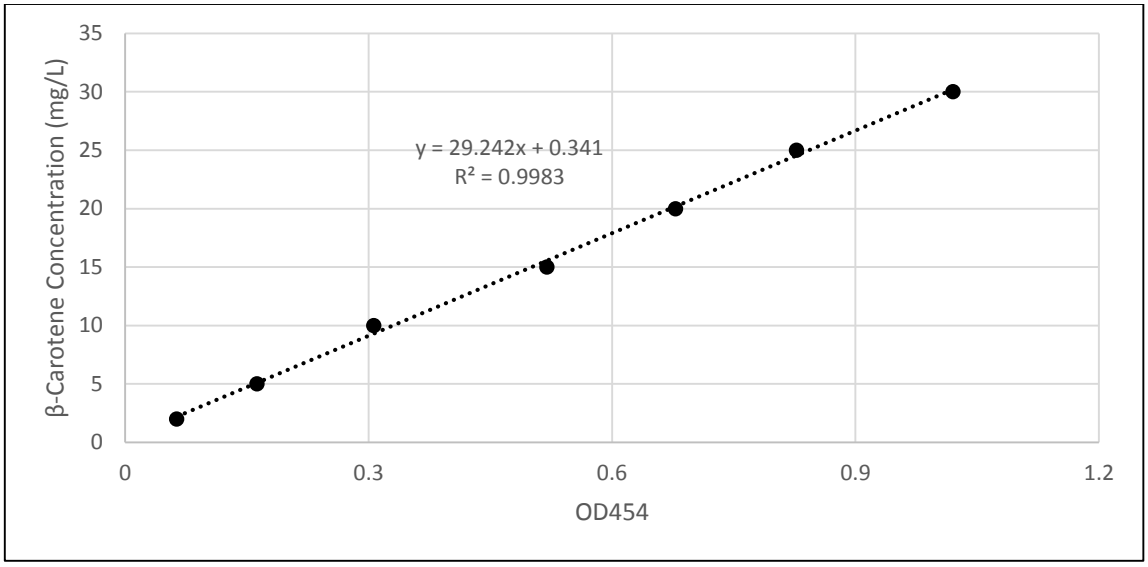

Figure 5. β-Carotene Standard Curve. Generated with β-Carotene obtained from Enzo Life Sciences.

Table 7. Total Carotenoid Secretion. Values are calculated from the area under the curve ranging from 350 nm to 550 nm wavelengths and normalized to the reference strain, SM14-ATA.

	Relative Carotenoid Secretion	**Standard Deviation**	**p-value**
SNQ2	1.179	0.227	0.06
STE6	0.715	0.136	0.004
YOR1	0.639	0.117	0.001